Aluminum Plasmonics for Enhanced Visible Light Absorption and High Efficiency Water Splitting in Core-Multishell Nanowire Photoelectrodes with Ultrathin Hematite Shells

Sarath Ramadurgam

Department of Physics and Astronomy, Purdue University

03/07/2014

Contents

Key Advantages and Challenges

Advantages:

- Ideal Bandgap (2.1 eV); good absorption in the visible range (250-600 nm)
- The theoretical maximum (1-sun) photocurrent density is 12.6 mA/cm^2 (solar to hydrogen conversion efficiency (STH) of 15.5%)[1-7]
- Valence Band ideal to catalyze oxygen evolution reaction
- Stable in aqueous medium, inexpensive and abundant

Challenges:

- Recombination due to short minority carrier diffusion length 20 nm i.e. poor Internal Quantum Efficiency (IQE)[7-9]
- Large requisite overpotential to drive hydrogen evolution reaction
- Poor reaction kinetics and high surface recombination

Plausible Solutions

- Nanostructures to improve absorption, reaction surface area and charge collection[2,3]; eg. Optical resonances in Nanowires[11-13]
- Best STH obtained by solving the surface reaction kinetics and absorption using co-catalysts, doping and nanowires is 5.3%[10].
- Plasmonic nanostructures, opal scaffolds and resonant light traps for concentrating light, enhance absorption and provide hot electrons[14-25]
- Best STH obtained by solving the surface reaction kinetics, absorption and overpotential using Au nanoparticles, Si-Hematite core-shell (CS) nanowires is 6%[18]
- Overpotential: Dual absorber systems eg. Si-Hematite [18, 31-33]

Motivation

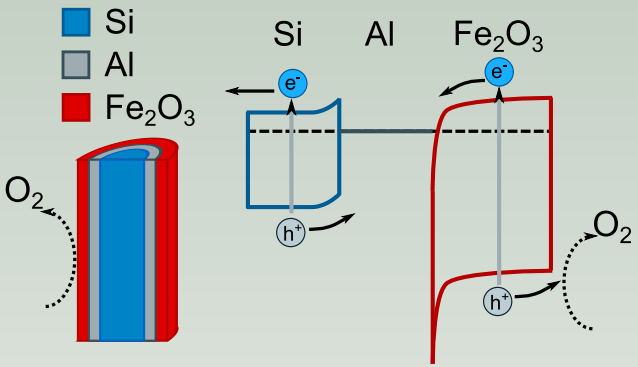

Figure: $Si - Al - Fe_2O_3$ Core-Multishell Nanowire Photoelectrodes: Schematic and Band-structure

- Alternative to plasmonic nanoparticles for enhanced absorption: metal-semiconductor core-shell nanowires and nanocones[26-28]
- Advantage: uniform field enhancement; size controllability
- Scalable Plasmonics?
- Al an alternative to precious metals: tunable LSPR in the UV-vis; strongly enhances fields; inexpensive and abundant; CMOS compatible

Our approach: *semiconductor-metal-metal oxide core-multishell (CMS) nanowires* can combine 1) optical resonances in nanowires, 2) LSPR in metal shell and 3) dual absorption into one integrated plasmonic structure

Solution to Maxwell's Equations

The rigerous solutions to Maxwell's Equations are obtained following the Mie-formalism[34-37].
Assumptions: 1) Nanowires are infinitely long ($length > 10 \times diameter$) and homogenous (optical constants obtained from ref. [7,38]), and 2) plane wave illumination ($e^{-i\omega t}$)

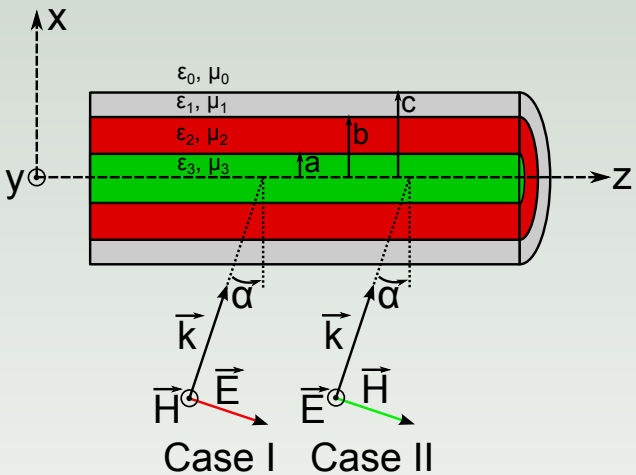

Figure: CMS nanowire under unpolarized oblique incidence.

The Maxwell's Equations (in SI units) are:

$$\nabla \times \vec{E} = i\omega\mu\vec{H} \tag{1a}$$

$$\nabla \times \vec{H} = -i\omega\epsilon\vec{E} \tag{1b}$$

$$\nabla \cdot (\epsilon\vec{E}) = 0 \tag{1c}$$

$$\nabla \cdot (\mu\vec{H}) = 0 \tag{1d}$$

To solve the scattering problem, we consider two polarizations of the incident light.

Solution to Maxwell's Equations

Assuming the nanowire is along the $\vec{z}$ axis, the scalar plane wave incidence is given as:

$$\psi = E_o e^{-i(fr+hz)} = E_o e^{-ihz} \sum_n i^{-n} J_n(fr) e^{in\phi} = \sum_n J_n(fr) F_n \tag{2}$$

Here, $h = k_0 \sin\alpha$ and $F_n = E_o i^{-n} e^{-ihz} e^{in\phi}$.
Let $V_n = A_n\psi$ and $U_n = B_n\psi$ be the solutions to the scalar wave equation ($\nabla^2\psi + k^2\psi = 0$). Now the fields can be expressed in terms of V_n and U_n as:

$$E_r = \sum_n \{ \tfrac{in}{r} V_n + \tfrac{ih}{k} \tfrac{\partial U_n}{\partial r} \} \tag{3a}$$

$$E_\phi = \sum_n \{ -\tfrac{\partial V_n}{\partial r} - \tfrac{nh}{kr} U_n \} \tag{3b}$$

$$E_z = \sum_n \{ \tfrac{f^2}{k} U_n \} \tag{3c}$$

$$H_r = \tfrac{k}{i\mu\omega} \sum_n \{ \tfrac{ih}{k} \tfrac{\partial V_n}{\partial r} + \tfrac{in}{r} U_n \} \tag{3d}$$

$$H_\phi = \tfrac{k}{i\mu\omega} \sum_n \{ -\tfrac{nh}{kr} V_n - \tfrac{\partial U_n}{\partial r} \} \tag{3e}$$

$$H_z = \tfrac{k}{i\mu\omega} \sum_n \{ \tfrac{f^2}{k} V_n \} \tag{3f}$$

At each interface we apply the boundary conditions for the continuity of E_ϕ, E_z, H_ϕ and H_z. The system of linear equations are solved to obtain the coefficients and the fields.

The meaning of 'n'

- Assume incidence perpendicular to nanowire axis. Case I - TM; Case II - TE
- For TM, n=0,2,4... corresponds to the electric dipolar, quadrapolar, multipolar terms; n=1,3,5... correspond to the magnetic dipolar, quadrapolar, multipolar terms.
- Similarly for TE, n=even is magnetic terms and n=odd is the electric terms.
- Optical resonances - strong dipolar terms.
- Double resonance (meta-atoms) - spectral overlap of n=0 and n=1 components

Absorption Efficiency

The total absorption and the scattering efficiencies for the CMS nanowire can be obtained from the coefficients as follows:

$$
\begin{aligned}
Q_{sca}^{(I)} &= \frac{2}{k_0 c}\{\sum_{n=-\infty}^{+\infty}(|a_n^{(I)}|^2 + |b_n^{(I)}|^2)\} \\
Q_{ext}^{(I)} &= \frac{2}{k_0 c}\{\sum_{n=-\infty}^{+\infty} Re(b_n^{(I)})\} \\
Q_{abs}^{(I)} &= Q_{ext}^{(I)} - Q_{sca}^{(I)} \\
Q_{sca}^{(II)} &= \frac{2}{k_0 c}\{\sum_{n=-\infty}^{+\infty}(|a_n^{(II)}|^2 + |b_n^{(II)}|^2)\} \\
Q_{ext}^{(I)} &= \frac{2}{k_0 c}\{\sum_{n=-\infty}^{+\infty} Re(a_n^{(II)})\} \\
Q_{abs}^{(II)} &= Q_{ext}^{(II)} - Q_{sca}^{(II)}
\end{aligned}
\tag{4}
$$

The scattering and absorption efficiencies for unpolarized light is obtained by:

$$
\begin{aligned}
Q_{abs} &= \tfrac{1}{2}\{Q_{abs}^{(I)} + Q_{abs}^{(II)}\} \\
Q_{sca} &= \tfrac{1}{2}\{Q_{sca}^{(I)} + Q_{sca}^{(II)}\}
\end{aligned}
\tag{5}
$$

Integrated Photon Flux Absorbed

The absorption efficiency within individual layers (η_i) is the ratio of the power absorbed over the power incident per unit length of the wire. The absorption efficiency is given as:

$$\begin{aligned}
\eta_i^{(I)} &= \frac{k_0}{2cE_0^2}\int\int Im\{\epsilon(r)\}|(E_r^{(I)})^2 + (E_\phi^{(I)})^2 + (E_z^{(I)})^2|r\,dr\,d\phi \\
\eta_i^{(II)} &= \frac{k_0}{2cE_0^2}\int\int Im\{\epsilon(r)\}|(E_r^{(II)})^2 + (E_\phi^{(II)})^2 + (E_z^{(II)})^2|r\,dr\,d\phi \\
\eta_i &= \tfrac{1}{2}\{\eta_i^{(I)} + \eta_i^{(II)}\}
\end{aligned} \tag{6}$$

In order to obtain absorption in eahc layer, the integration limits in (6) are set accordingly.
The integrated photon flux absorbed ($\Phi_{abs,i}$) within each layer is obtained as follows:

$$\Phi_{abs,i} = \int_{\lambda_1=300nm}^{\lambda_2=590nm} \frac{\lambda}{h_{Planck}c_{light}} I_{AM1.5G}(\lambda)\eta_i\,d\lambda \tag{7}$$

Spatial Distribution of the Photon Flux Absorbed

$$\chi_{abs,i}(r,\phi) = \int_{\lambda_1=300nm}^{\lambda_2=590nm} \frac{\lambda}{h_{Planck}c_{light}} I_{AM1.5G}(\lambda) \frac{k_0}{2cE_0^2} \frac{Im\{\epsilon(r)\}}{2} \{|(E_r^{(I)})^2 + (E_\phi^{(I)})^2 + (E_z^{(I)})^2| + |(E_r^{(II)})^2 + (E_\phi^{(II)})^2 + (E_z^{(II)})^2|\}\, d\lambda \tag{8}$$

Note, the total photon flux absorbed is just the area integral of the spatial distribution. The units of $\chi_{abs,i}(r,\phi)$ is *photons* cm^{-2} s^{-1}.

Integrated Photon Flux Absorbed

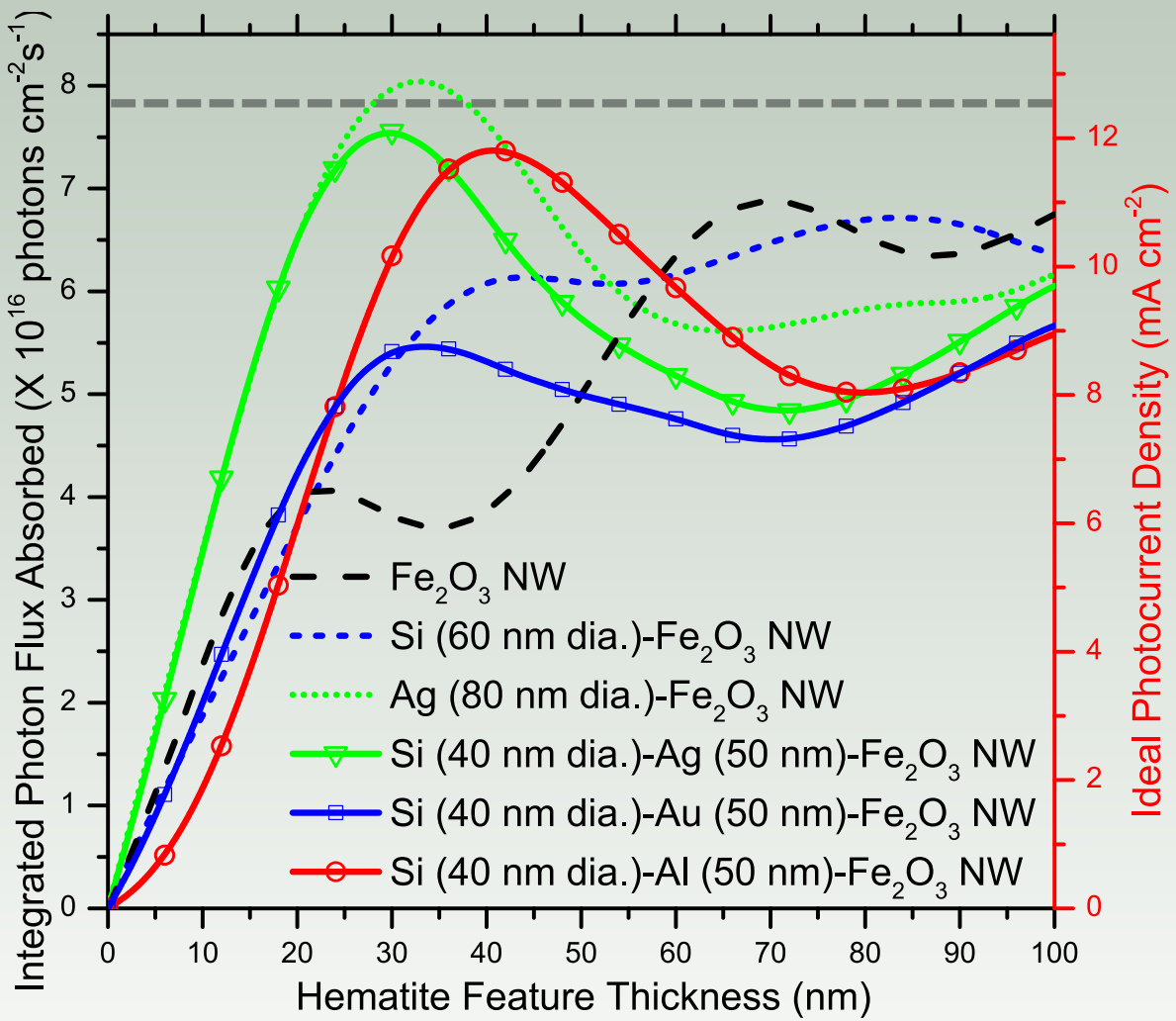

Figure: Integrated absorbed photon flux($\Phi_{abs,i}$) and ideal photocurrent density ($J = q\Phi_{abs,i}$) under within the hematite shell for various NW structures 1-sun illumination incident normal to the NW axis. The grey dashes indicate the theoretical maximum absorption in bulk hematite.

Integrated Photon Flux Absorbed (Supporting Information)

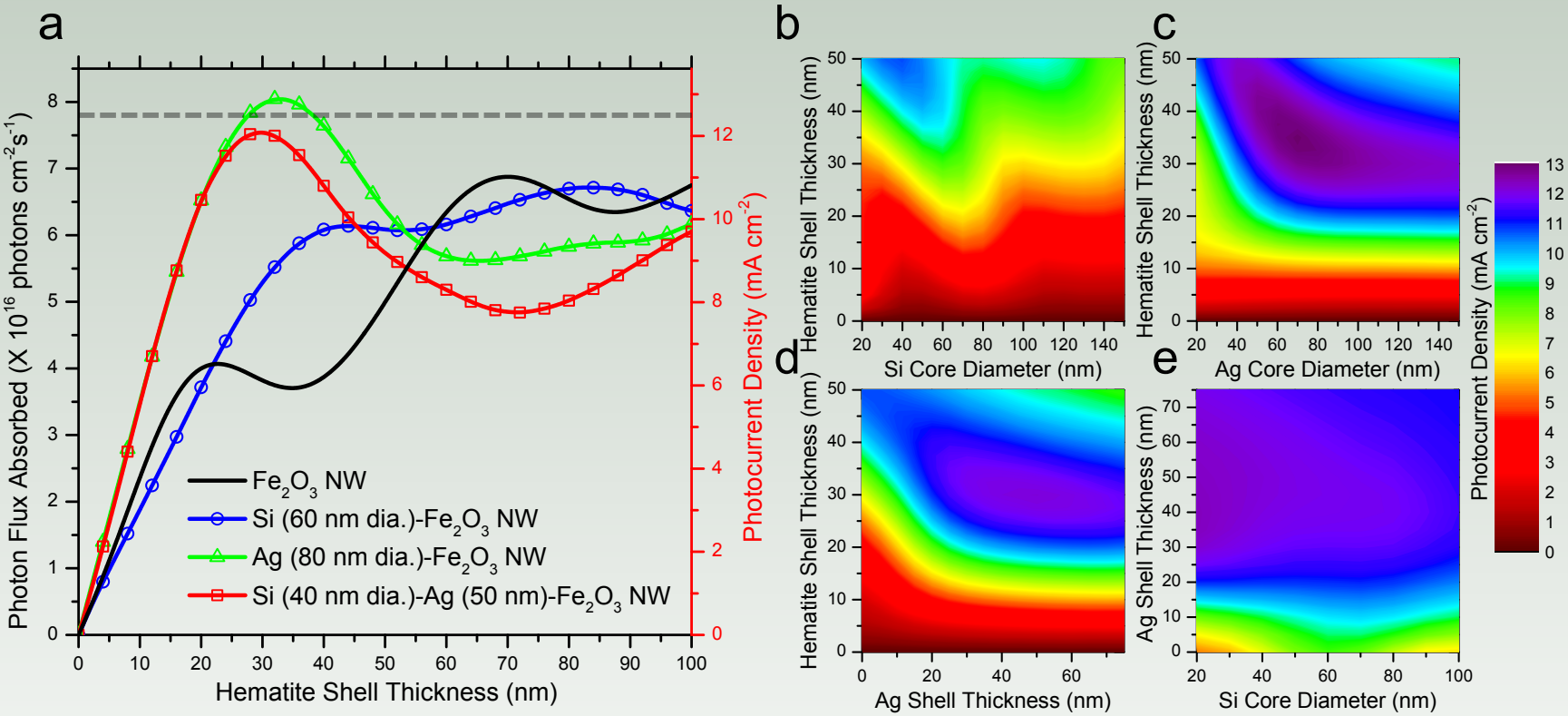

Figure: a) Integrated photon flux absorbed and the corresponding ideal photocurrent density versus the hematite shell thickness for core-shell and core-multishell nanowires.Ideal photocurrent density contours plotted for b) $Si - Fe_2O_3$, c) $Ag - Fe_2O_3$, d) $Si(40nmdia.) - Ag - Fe_2O_3$ and e) $Si - Ag - Fe_2O_3(30nm)$ nanowires.

Absorption Efficiency of 'Ideal' Structures

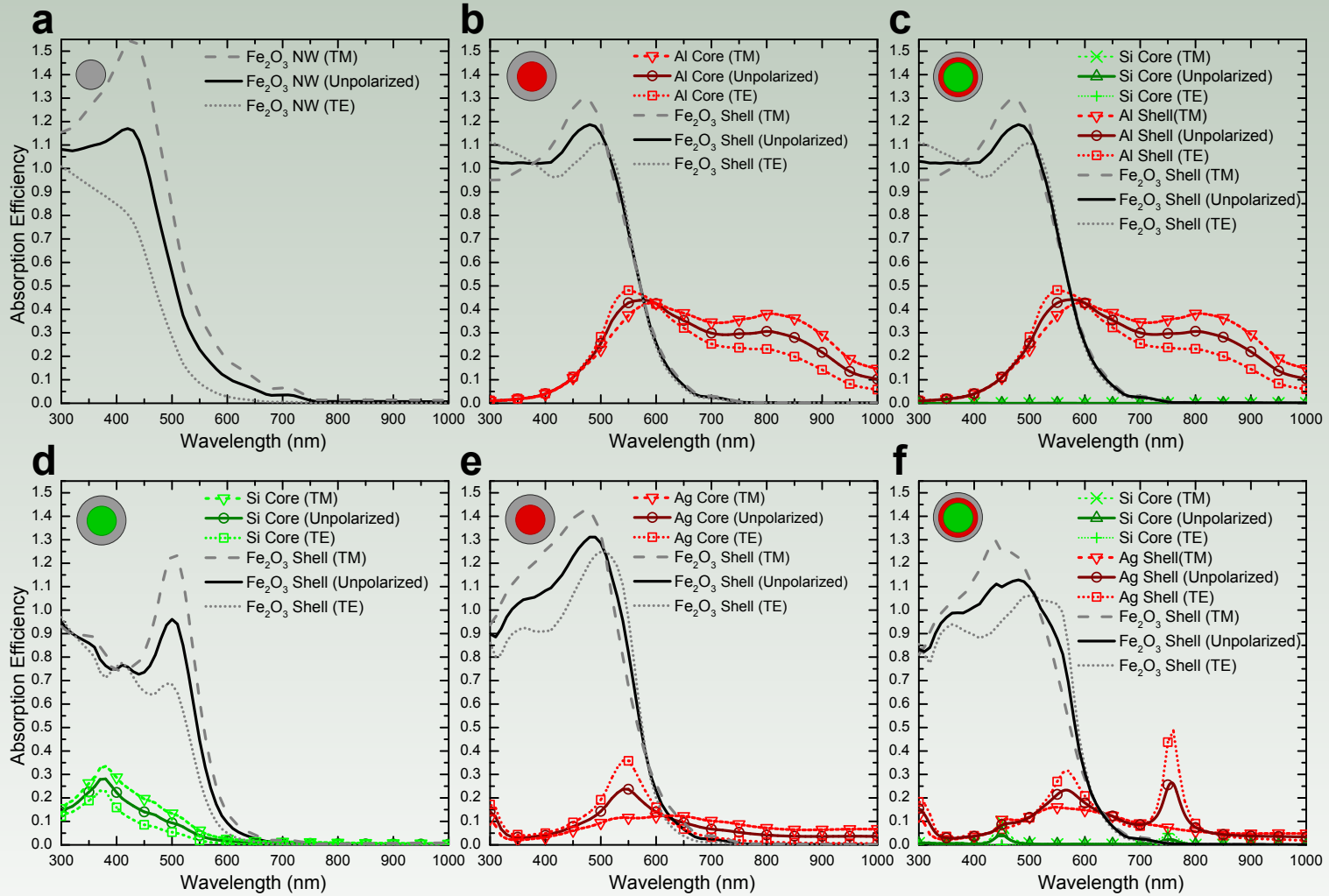

Figure: The absorption efficiency under TE, TM and unpolarized illumination as a function of wavelength plotted for individual core and shell layers of (a) $Fe_2O_3(100\ nm\ dia.)$, (b) $Al(140\ nm\ dia.) - Fe_2O_3(40\ nm)$ CS, (c) $Si(40\ nm\ dia.) - Al(50\ nm) - Fe_2O_3(40\ nm)$ CMS, (d) $Si(60\ nm\ dia.) - Fe_2O_3(30\ nm)$ CS, (e) $Ag(80\ nm\ dia.) - Fe_2O_3(30\ nm)$ CS and (f) $Si(40\ nm\ dia.) - Ag(50\ nm) - Fe_2O_3(30\ nm)$ CMS NW.

Effectiveness of the Dual Absorber System

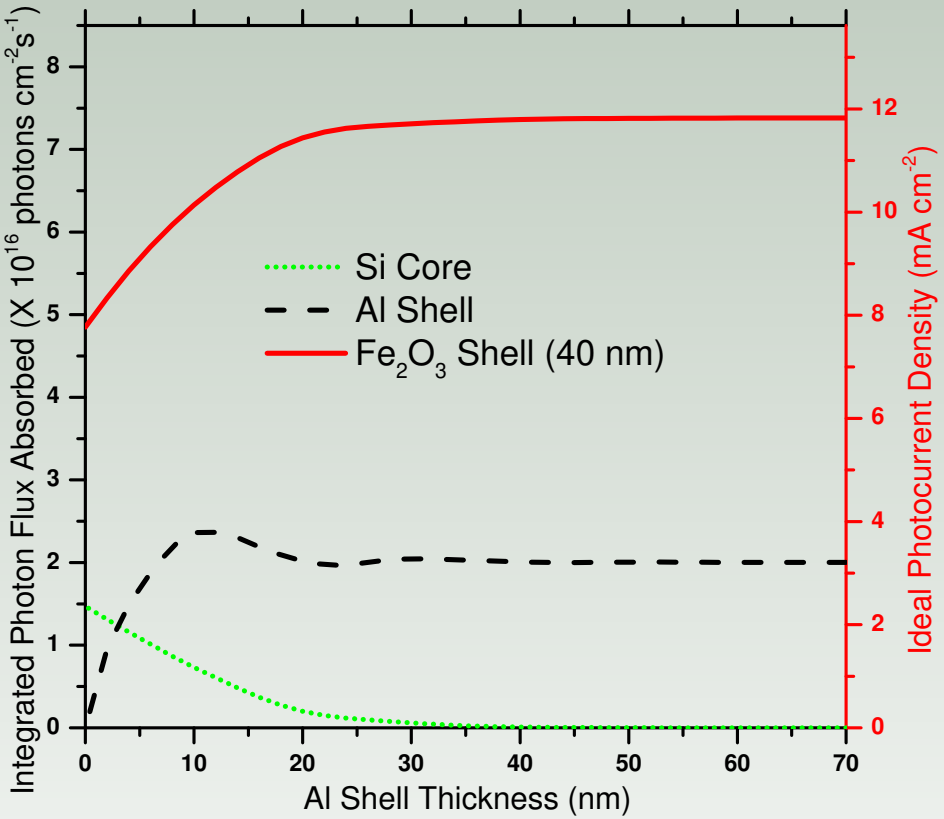

Figure: The integrated photon flux absorbed within the *Si* core (green dots), *Al* intermediate shell (black dashes) and Fe_2O_3 outer shell (red line) of a $Si - Al - Fe_2O_3$ CMS NW. The total nanowire radius is fixed at 110 *nm*, the Fe_2O_3 thickness is fixed at 40 *nm* and the *Al* thickness is varied (i.e. *Si radius* $= 70\ nm -$ *Al thickness*).

- Critical thickness of the Al shell is about 25 nm
- Si core does not show appreciable absorption
- Si wafer in large area devices would absorb substantially
- Wafer absorption can be tuned by adjusting inter-nanowire distances
- Si nanowires act as scaffolds for the subsequent shell layers

Spatial Distributiong of The Absorbed Photon Flux

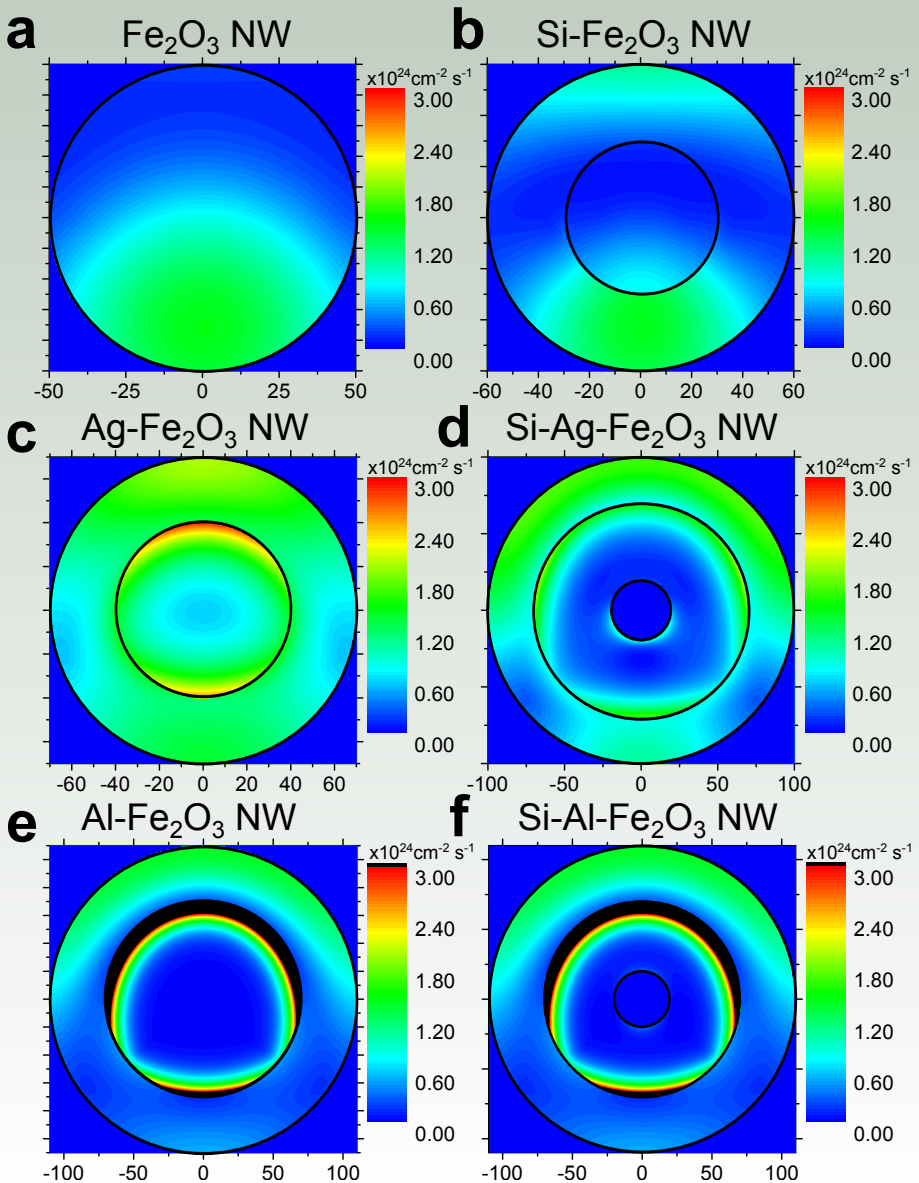

The spatial distribution of the absorbed photon flux under unpolarized illumination plotted for various 'ideal' NW structures.
Note: The color scales have been fixed for easier comparison. The peak photon flux absorbed in $Si - Al - Fe_2O_3$ CMS NW (regions in black) is about 5 times larger than $Si - Ag - Fe_2O_3$ CMS NW

Effect of Incident Angle and Polarization

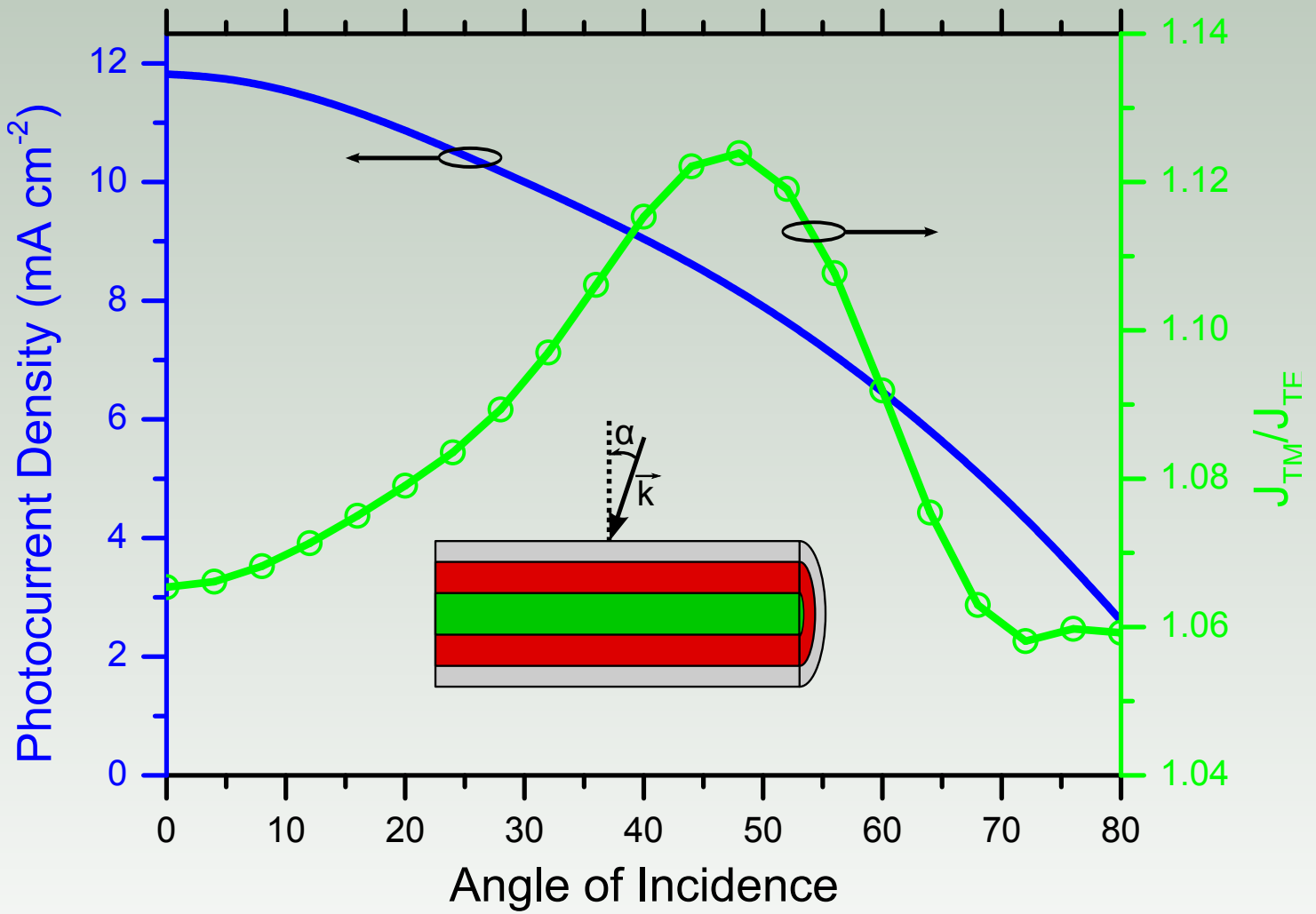

Figure: The ideal photocurrent density (blue) and the ratio of the photocurrent density under TM and TE illumination (green) as a function of the incident angle within the hematite shell of a $Si(40\ nm\ dia.) - Al(50\ nm) - Fe2O3(40\ nm)$ CMS NW. Inset: Schematic of CMS nanowire under oblique incidence.

Conclusions

- $Si - Al - Fe_2O_3$ CMS NWs exhibit strong absorption enhancement in sub-50 nm hematite shells
- Charges are typically generated very close to the electrolyte interface and hence are expected to exhibit minimal recombination thereby improving the Internal Quantum Efficiency
- Al is an excellent alternative plasmonic material to precious metals in such CMS structures
- Although the NW geometry is highly anisotropic, the CMS NWs have been shown to be highly isotropic
- Under ideal conditions, a high photocurrent density is predicted for incidence angles as large as 45°
- Si NWs as a scaffolds and Al thin films as shells offers greater control over the material quality and thickness, as compared to plasmonic nanoparticles based designs
- The Si wafer in large scale devices is expected to effectively contribute towards 'dual absorption' and hence reduce the overpotential
- Al based CMS architecture is very general and hence is expected to provide similar absorption enhancement in other photocatalyst materials beyond hematite

1. Bak T, Nowotny J, Rekas M, Sorrell C. Photo-electrochemical hydrogen generation from water using solar energy. Materials-related aspects. Int J Hydrogen Energy 2002, 27: 991-1022.
2. van de Krol R, Liang Y, Schoonman J. Solar hydrogen production with nanostructured metal oxides. J Mater Chem 2008, 18: 2311.
3. Sun J, Zhong DK, Gamelin DR. Composite photoanodes for photoelectrochemical solar water splitting. Energy Environ Sci 2010, 3: 1252.
4. Chen Z, Jaramillo TF, Deutsch TG, Kleiman-Shwarsctein A, Forman AJ, Gaillard N, et al. Accelerating materials development for photoelectrochemical hydrogen production: Standards for methods, definitions, and reporting protocols. J Mater Res 2011, 25: 3-16.
5. Sivula K, Le Formal F, Grätzel M. Solar water splitting: progress using hematite (?-Fe(2) O(3)) photoelectrodes. ChemSusChem 2011, 4: 432-449.
6. Katz MJ, Riha SC, Jeong NC, Martinson ABF, Farha OK, Hupp JT. Toward solar fuels: Water splitting with sunlight and "rust"? Coord Chem Rev 2012, 256: 2521-2529.
7. Dotan H, Kfir O, Sharlin E, Blank O, Gross M, Dumchin I, et al. Resonant light trapping in ultrathin films for water splitting. Nat Mater 2013, 12: 158-164.
8. Dare-Edwards M, Goodenough J, Hamnett A, Trevellick P. Electrochemistry and photoelectrochemistry of iron (III) oxide. J Chem Soc Faraday Trans 1983, 79: 2027-2041.
9. Dotan H, Sivula K, Grätzel M, Rothschild A, Warren SC. Probing the photoelectrochemical properties of hematite (?-Fe2O3) electrodes using hydrogen peroxide as a hole scavenger. Energy Environ Sci 2011, 4: 958.
10. Kim JY, Magesh G, Youn DH, Jang J-W, Kubota J, Domen K, et al. Single-crystalline, wormlike hematite photoanodes for efficient solar water splitting. Sci Rep 2013, 3: 2681.
11. Cao L, White JS, Park J-S, Schuller Ja, Clemens BM, Brongersma ML. Engineering light absorption in semiconductor nanowire devices. Nat Mater 2009, 8: 643-647.
12. Cao L, Fan P, Vasudev AP, White JS, Yu Z, Cai W, et al. Semiconductor nanowire optical antenna solar absorbers. Nano Lett 2010, 10: 439-445.
13. Yu Y, Ferry VE, Alivisatos aP, Cao L. Dielectric core-shell optical antennas for strong solar absorption enhancement. Nano Lett 2012, 12: 3674-3681.
14. Thimsen E, Le Formal F, Grätzel M, Warren SC. Influence of plasmonic Au nanoparticles on the photoactivity of Fe2O3 electrodes for water splitting. Nano Lett 2011, 11: 35-43.
15. Thomann I, Pinaud Ba, Chen Z, Clemens BM, Jaramillo TF, Brongersma ML. Plasmon enhanced solar-to-fuel energy conversion. Nano Lett 2011, 11: 3440-3446.
16. Gao H, Liu C, Jeong HE, Yang P. Plasmon-enhanced photocatalytic activity of iron oxide on gold nanopillars. ACS Nano 2012, 6: 234-240.
17. Li J, Cushing SK, Zheng P, Meng F, Chu D, Wu N. Plasmon-induced photonic and energy-transfer enhancement of solar water splitting by a hematite nanorod array. Nat Commun 2013, 4: 2651.
18. Wang X, Peng K, Hu Y, Zhang F, Hu B. Silicon/Hematite Core/shell Nanowire Array Decorated with Gold Nanoparticles for Unbiased Solar Water Oxidation. Nano Lett 2013: 1-8.

19. Riha SC, Klahr BM, Tyo EC, Seifert S, Vajda S, Pellin MJ, et al. Atomic layer deposition of a submonolayer catalyst for the enhanced photoelectrochemical performance of water oxidation with hematite. ACS Nano 2013, 7: 2396-2405.
20. Schuller Ja, Barnard ES, Cai W, Jun YC, White JS, Brongersma ML. Plasmonics for extreme light concentration and manipulation. Nat Mater 2010, 9: 193-204.
21. Cushing S, Li J, Meng F. Photocatalytic activity enhanced by plasmonic resonant energy transfer from metal to semiconductor. J Am Chem Soc 2012, 134: 15033-15041.
22. Linic S, Christopher P, Ingram DB. Plasmonic-metal nanostructures for efficient conversion of solar to chemical energy. Nat Mater 2011, 10: 911-921.
23. Warren SC, Thimsen E. Plasmonic solar water splitting. Energy Environ Sci 2012, 5: 5133.
24. Mubeen S, Lee J, Singh N, Krämer S, Stucky GD, Moskovits M. An autonomous photosynthetic device in which all charge carriers derive from surface plasmons. Nat Nanotechnol 2013, 8: 247-251.
25. Mukherjee S, Libisch F, Large N. Hot electrons do the impossible: Plasmon-induced dissociation of H2 on Au. Nano Lett 2013, 13: 240-247.
26. Zhan Y, Zhao J, Zhou C, Alemayehu M, Li Y, Li Y. Enhanced photon absorption of single nanowire ?-Si solar cells modulated by silver core. Opt Express 2012, 20: 11506-11516.
27. Mann SA, Garnett EC. Extreme light absorption in thin semiconducting films wrapped around metal nanowires. Nano Lett 2013, 13: 3173-3178.
28. Zhou L, Yu X, Zhu J. Metal-Core/Semiconductor-Shell Nanocones for Broadband Solar Absorption Enhancement. Nano Lett 2014.
29. Knight MW, Liu L, Wang Y, Brown L, Mukherjee S, King NS, et al. Aluminum plasmonic nanoantennas. Nano Lett 2012, 12: 6000-6004.
30. Knight MW, King NS, Liu L, Everitt HO, Nordlander P, Halas NJ. Aluminum for Plasmonics. ACS Nano 2013.
31. Mayer MT, Du C, Wang D. Hematite/Si nanowire dual-absorber system for photoelectrochemical water splitting at low applied potentials. J Am Chem Soc 2012, 134: 12406-12409.
32. Du C, Yang X, Mayer MT, Hoyt H, Xie J, McMahon G, et al. Hematite-Based Water Splitting with Low Turn-On Voltages. Angew Chem Int Ed 2013, 52: 12692-12695.
33. van de Krol R, Liang Y. An n-Si/n-Fe2O3 heterojunction tandem photoanode for solar water splitting. Chimia 2013, 67: 168-171.
34. Kerker M, Matijevic E. Scattering of Electromagnetic Waves from Concentric Infinite Cylinders. J Opt Soc Am 1961, 51: 506-508.
35. Lind AC. Electromagnetic Scattering by Obliquely Oriented Cylinders. J Appl Phys 1966, 37: 3195.
36. Shah G. Scattering of plane electromagnetic waves by infinite concentriccircular cylinders at oblique incidence. Mon Not R Astr Soc 1970, 148: 93-102.
37. Bohren C, Huffman D. Absorption and scattering of light by small particles. Wiley-VCH, 2004.
38. Ni X, Liu Z, Kildishev A. PhotonicsDB: Optical Constants, 2010.